Quantification of Early Diffuse Myocardial Fibrosis Through 7.0 T Cardiovascular Magnetic Resonance T1 Mapping in a Type 1 Diabetic Mellitus Mouse Model

Hongkai Zhang
Beijing An Zhen Hospital: Capital Medical University Affiliated Anzhen Hospital https://orcid.org/0000-0001-6191-5106
Chun-Yan Shi
Beijing An Zhen Hospital: Capital Medical University Affiliated Anzhen Hospital
Lin Yang
Beijing An Zhen Hospital: Capital Medical University Affiliated Anzhen Hospital
Nan Zhang
Beijing An Zhen Hospital: Capital Medical University Affiliated Anzhen Hospital
Guo-qi Li
Beijing Institute of Heart Lung and Blood Vessel Diseases: Capital Medical University Affiliated Anzhen Hospital
Zhen Zhou
Beijing An Zhen Hospital: Capital Medical University Affiliated Anzhen Hospital
Yi-feng Gao
Beijing An Zhen Hospital: Capital Medical University Affiliated Anzhen Hospital
Dong-ting Liu
Beijing An Zhen Hospital: Capital Medical University Affiliated Anzhen Hospital
Lei Xu (leixu2001@hotmail.com)
Beijing An Zhen Hospital: Capital Medical University Affiliated Anzhen Hospital https://orcid.org/0000-0002-8499-0448
Zhan-ming Fan
Beijing An Zhen Hospital: Capital Medical University Affiliated Anzhen Hospital

Original investigation

Keywords: Diffuse myocardial interstitial fibrosis, Diabetic cardiomyopathy, Cardiac magnetic resonance imaging, T1 mapping and ECV, Collagen volume fraction

Posted Date: May 11th, 2021

DOI: https://doi.org/10.21203/rs.3.rs-479417/v1

Abstract

Background Diffuse myocardial interstitial fibrosis (DMIF) is a key factor for heart failure (HF) in diabetic cardiomyopathy. This study examined the accuracy of the qualitative and quantitative evaluation of early DMIF in a type 1 diabetes mellitus (T1DM) mouse model through 7.0 T cardiac magnetic resonance imaging-based T1 mapping.

Methods Eight-week-old C57Bl/6J male mice were randomly divided into control (n = 20) and T1DM (n = 30, induced by a low dose streptozotocin dose of 60 mg/kg) groups. The progression of DMIF was examined every 4 weeks until 24 weeks after successful establishment of the model. Cardiac functional and morphological parameters were evaluated through echocardiography by using a high-resolution ultrasound cardiovascular system. A 7.0 T CMR scan was performed using the pre- and post-contrast GRE Look–Locker inversion recovery T1 mapping sequence. The extracellular volume fraction (ECV) was calculated from CMR and hematocrit data. Sirius Red staining was simultaneously performed in each group to detect DMIF and calculate the collagen volume fraction (CVF). Differences in ECV and CVF values between two groups were analyzed using one-way analysis of variance. The correlation between ECV and CVF values was assessed using the Pearson test.

Results Six mice were included every 4 weeks in the control and T1DM groups for statistical analysis. Compared with the control group, a progressive decrease in FS, EF, and E/A ratio was observed in the T1DM group. In the T1DM group, both ECV and CVF values were gradually increased during diabetes progression. A marked increase in ECV and CVF values was observed at 12 weeks in the T1DM group than in the control group (ECV: 32.5% ± 1.6% vs 28.1% ± 1.8%, P = 0.002; CVF: 6.9% ± 1.8% vs 3.3% ± 1.1%, P < 0.01). ECV values showed a strong correlation with CVF in the T1DM group (r = 0.856, P < 0.001).

Conclusion ECV is a reliable and feasible imaging marker that can be used to quantitatively assess dynamic DMIF changes in T1DM mice. In addition, ECV could accurately detect DMIF in the early stage and thus can be used as an imaging tool for early intervention in T1DM mice in the future.

Introduction

Diabetes mellitus (DM) is one of the most common chronic diseases in humans. DM is an independent risk factor for different cardiovascular diseases (CVDs), particularly heart failure (HF)[1, 2]. In 1974, Hamby et al. first described diabetic cardiomyopathy (DCM)[3], which is the most common complication of DM. In addition, DCM is a major cause of mortality in patients with DM. DCM can be divided into early, middle, and late stages according to changes in molecular levels and heart structure and function[4]. Therefore, early DCM diagnosis and appropriate intervention are crucial for reducing mortality.

Myocardial fibrosis (MF) is typically characterized by an increased cardiac extracellular matrix, which is a common pathological change in most CVDs[5, 6]. MF mainly includes replacement and diffuse fibrosis. Cardiac magnetic resonance (CMR) late gadolinium enhancement (LGE) imaging is considered the “gold standard” for accurately detecting regional MF[7]. However, this imaging technique cannot identify diffuse myocardial interstitial fibrosis (DMIF) because it does not compare the signal intensity between the normal myocardium and fibrotic myocardium, thus resulting in false negative findings[8]. DMIF is the main pathological process of DCM, leading to ventricular remodeling and dysfunction[1, 2].

The CMR T1 mapping technique can quantitatively evaluate DMIF by measuring the pre- and post-contrast T1 values of the myocardium (by using gadolinium–diethylenetriaminepentaacetic acid) and calculating the extracellular volume fraction (ECV)[9]. ECV reflects the degree of diffuse myocardial fibrosis. To verify the effectiveness of the T1 mapping technique in evaluating early DMIF in vivo, we performed dynamic CMR imaging at multiple time points in a streptozotocin (STZ)-induced DM mouse model[10–12]. The use of this mouse model in clinical research has helped prevent multiple complications such as complicated hypertension and complicated ischemic cardiomyopathy. In this mouse model, images can be obtained at any time point, and molecular, biochemical, and histological examinations can be performed to evaluate the DCM duration.

The present study examined whether in vivo T1 mapping techniques (particularly ECV calculation) can effectively assess dynamic DMIF changes in type 1 DM (T1DM) mice, especially the accurate detection of DMIF in the early stage.

Materials And Methods

Animals and experimental models

Fifty 8-week-old C57Bl/6J male mice were used in this study. The mice were randomly divided into two groups: T1DM (n = 30) and control (n = 20) groups. All the mice were individually fed under a 12–12-h light–dark cycle in standard laboratory conditions at constant temperature and 60% humidity. They were provided food and water ad libitum. Experimental procedures performed in mice were approved by the Ethics Committee of Laboratory Animals at the Capital Medical University of China.

Mice in the T1DM group were fed a normal diet (containing 10% kcal fat D12450B, Research Diets, New Brunswick, USA). STZ (Sigma Aldrich, Budapest, Hungary) was diluted in citric acid buffer (pH = 4.5, 10 mg/mL). Subsequently, the mice were intraperitoneally injected with a low dose of STZ (60 mg/kg in citric acid buffer) for five consecutive days[12]. Meanwhile, mice in the control group received only the same volume of citric acid buffer. Five days after the injection of STZ, mice with a blood glucose level of ≥13.9 mmol/L were considered to be diabetic[12, 13]. Normal diet was fed in the control and T1DM groups continuously.

Echocardiography

Before magnetic resonance imaging (MRI), echocardiography was performed using a high-resolution ultrasound cardiovascular system (VEVO 2100, VisualSonics, Canada) with a 15–20-MHz linear transducer. Isoflurane anesthesia (with 1%–2% isoflurane in 100% oxygen) was administered, and mice were placed on a thermal regulation board in supine position at 37 °C. Images were analyzed using the VEVO Lab Version-3.1.1 ultrasound workstation. Left ventricular (LV) long axis and mid-papillary level short axis with the M-mode were used to determine the heart rate and measure LV mass, fractional shortening (FS), and ejection fraction (EF). Parameters related to diastolic function were measured. Early (E) and late (A) diastolic peak velocities and the ratio of E/A were examined using the mitral valve inflow pattern. All values were averaged across three cardiac cycles[14].

MRI

Animals were anesthetized using isoflurane (2% induced concentration and 1% maintained concentration) and scanned under a 7.0T MRI system (Varian, R 16, USA) by using a 4-channel phased-array mouse heart coil (Varian, USA, Fig. 1A). Before each scan, blood samples were collected from the tail of each mouse to perform hematocrit (HCT) examination. The CMRI protocol is shown in Fig. 1B. Pre-T1 mapping images were acquired in the prone position. A contrast agent (0.5 mmol/kg, Gd-DTPA, Bayer Phamar AG) was intraperitoneally injected. Fifteen minutes after the contrast injection, LGE-MRI was performed using a multi-slice inversion recovery sequence[15]. Subsequently, post-T1 mapping was conducted 30 min after Gd-DTPA injection by using by a 3-slice GRE look–locker inversion recovery sequence to acquire the true short-axis images at the end diastole[16]. T1 mapping parameters were as follows: slice thickness, 1 mm, field of view, 25.6 × 25.6 mm, data matrix, 128 × 128, time of repetition, 6.5 ms, echo time, 3.3 ms, flip angle, 20°, inversion time, 45, and excitation pulse, 15°. The acquisition time was approximately 8 s per slice to allow full relaxation.

All data were manually analyzed in a blinded manner by using VnmrJ4.0 (Varian, USA) postprocessing software. A region of interest (ROI) was defined in the LV myocardium and blood pool to assess pre- and post-contrast T1 values in the basal, mid, and apical slices. ECV was calculated as follows: ECV = (1 − hematocrit) × (ΔR1 myocardium/ΔR1 blood), where R1 = 1/T1[16, 17]. To prevent partial volume effects and blood pool contamination, we performed T1 mapping analysis by using the ROI in the middle myocardium.

Histopathological analysis

A solution of 10% formalin was used to fix the myocardium. In particular, the pathological sections of the ventricular septum myocardium corresponding to the MRI scanning area were selected. Then, 5-μm-thin myocardial slices were subjected to conventional histology (hematoxylin–eosin and Sirius Red) staining. Sirius Red staining was performed to detect collagen deposition and calculate the collagen volume fraction (CVF). Images were analyzed using NIS-Elements 4.10 software (Nikon, Japan).

Statistical Analysis

All statistical analyses were performed using GraphPad Prism, version 6.0 (GraphPad Software, San Diego, CA). Data are presented as the mean ± standard deviation. Homogeneity of variance was examined using Brown–Forsythe and Bartlett tests. Differences between groups were analyzed using one-way analysis of variance (ANOVA). Correlations between the two variables were assessed using Pearson's test. For comparisons, a P value of <0.05 was considered statistically significant.

Results

Animal models and characteristics

We monitored body weight and 3-h no-fasting blood glucose levels in the T1DM and control groups before and after diabetes onset (Fig. 1C and 1D). Compared with the control group, the average body weight decreased in the T1DM group (Fig. 1C). Blood glucose levels increased in the T1DM group (Fig. 1D).

Cardiac morphology and echocardiographyfindings

The morphology and function of the LV (Fig. 2A) were assessed through conventional echocardiography in the T1DM and control groups (Table 1). We observed a gradual decrease from 8 weeks in the E wave and E/A ratio and a significant increase in the A wave from 12 weeks onward compared with baseline ($P < 0.05$, Table 1), suggesting diastolic dysfunction. We selected a few key variables from 12 weeks and compared them with baseline (Fig. 2B–F). In terms of systemic variables, EF and FS progressively decreased in the T1DM group from day 4 and significantly differed from baseline from 16 weeks onward (Table 1, Fig. 2C,D). In terms of structural variables, LV mass and LV mass (corrected) significantly increased from 12 weeks onward (Fig. 2E and F), suggesting potential hypertrophy of the heart.

CMR

No evidence of focal late contrast enhancement was noted in any DM group (Fig. 3A). T1 measurements were performed in the blood pool and heart of pre- and post-contrast GRE inversion recovery look–locker acquisitions. CMR T1 mapping parameters are shown in Fig. 3. The precontrast T1 myocardium values increased in the DM group only at 20 and 24 weeks (Fig. 3B), whereas a significant difference in postcontrast T1 myocardium values was observed between the T1DM and control groups from 12 weeks onward (Fig. 3C). ECV significantly differed between the T1DM and control groups (T1DM: 32.5% ± 1.6% vs. 28.1% ± 1.8%, $P = 0.002$) at 12 weeks (Fig. 3D). No significant change in HCT was observed between the T1DM and control groups (Fig. 3E).

Histological analysis of MF

The heart weight (Fig. 4A) and the ratio of heart weight/tibia length (Fig. 4B) were significantly increased in the T1DM group compared with the control group from 12 weeks and 8 weeks of diabetes, respectively. This index of heart hypertrophy supports the LV mass increase (Fig. 2E and F). Heart sections stained with Sirius red showed the progressive induction of extensive fibrosis throughout the myocardium in the T1DM group (Fig. 4C), for instance, at 12 weeks, CVF values significantly differed between the T1DM and control groups (T1DM: 6.9% ± 1.8% vs. 3.3% ± 1.1%, $P < 0.01$).

Correlation of CMR T1 mapping variables with E/A ratio and CVF

The ratio of E/A was significantly and negatively correlated with ECV (Fig. 5A).We observed a moderate positive correlation between precontrast T1 myocardium time (Fig. 5B) or postcontrast T1 myocardium time (Fig. 5C) and CVF. In addition, a strong positive correlation was noted between ECV and CVF (Fig. 5D).

Discussion

In this study, we performed a continuous evaluation through histological verification, CMR T1 mapping, and echocardiography parameters at longitudinal multi-time points in the T1DM mouse model. Meanwhile, the main objective was to determine the accuracy of the qualitative and quantitative evaluation of early DMIF at early time points. Our study results revealed that (a) the ECV value gradually increased during diabetic progression. Notably, at the 12-week time point, the ECV value significantly differed between the T1DM and control group. (b) The ECV value was strongly correlated with the CVF and moderately correlated with precontrast and postcontrast T1 values, which could continuous reflect the degree of DMIF in the duration of diabetes.

Because the myocardial T1 value was obtained to indirectly determine the tissue characteristics of the normal or damaged myocardium in humans, endomyocardial biopsy has seldom been performed in most cases, and the accuracy was still unstable[18]. Meanwhile, the accuracy was easily affected by CMR equipment, hemodynamics condition, acquisition sequence, and time phase. In addition, it was difficult to dynamically monitor cardiac diseases at multiple time points in humans[19] due to time and space. Thus, the underlying mechanism of disease progression remains unclear. However, animal models can be used to evaluate the degree of myocardial fibrosis by changing the T1 mapping parameter duration of DCM. Notably, not only the diabetic mouse model had the advantages of simplicity, high consistency, and excellent repeatability but also the effects of age, disease progression, and concomitant disease were prevented including those of hypertension[16] and coronary heart disease[20]. In this study, a diabetic mouse model was used, and DMIF was continuously monitored using a 7.0 T MRI device by using the GRE look–locker sequence compared with histology and echocardiography results.

Because the heart and respiratory rates of diabetic mice are affected by various factors (such as the flow concentration of the gas anesthetic, the severity of the disease, and ambient temperature), the changes are substantial[21]. Thus, cardiac tissue features are challenging to be accurately described. Transthoracic echocardiography is the most common imaging method that can assess the morphology and function of the heart, complying with the merits of no radiation and economic efficiency[22]. In our study, high-resolution echocardiography exhibited that compared with the control group, the T1DM group showed a gradual decrease in the E/A ratio. FS and EF progressively decreased in the T1DM group from 4 to 24 weeks, whereas EF was preserved; FS and EF values significantly differed at 16 weeks, whereas the E/A ratio significantly differed at 12 weeks between the T1DM and control groups. Diastolic dysfunction occurred earlier than systolic dysfunction, and the diastolic function gradually deteriorated in the T1DM group; this finding is consistent with that of previous studies[14, 23]. Meanwhile, LV mass and LV mass (corrected) increased from 4 to 24 weeks in the T1DM group, possibly due to cardiac hypertrophy, which was also confirmed by the increased ratio of the heart weight to tibia length.

CMRI not only has the advantages of no radiation and excellent repeatability but also can better evaluate the characteristics of the myocardium compared with echocardiography[6, 24]. Although the imaging time is considerably long, it is widely used to assess ischemic cardiomyopathy and nonischemic cardiomyopathy[25, 26]. DCM is mainly manifested as DMIF in the early stage of DM[4, 27]. In our experimental study, no LGE regions were observed in the myocardium in the T1DM group. Meanwhile, Zhang[28] and Zeng[29] have reported the same result. Some studies have indicated the presence of LGE regions in some patients with DM. Other mixed factors may lead to focal MF including nondiagnosed coronary heart disease, valvular heart diseases, and myocardial metabolic diseases[30].

In recent years, ultra-high field MRI and T1 mapping parameters have been widely used to detect DMIF[31, 32]. In particular, ECV can exhibit pre- and post-contrast T1 values when myocardial cells and blood pool contrast agents reach an equilibrium state. In addition, ECV can reflect changes in the myocardial extracellular matrix and is a relatively stable imaging marker that has been used to quantitatively evaluate DMIF. ECV is not disturbed by the acquisition time window, HCT, renal excretion rate, and contrast agent wash in and wash out in pathological conditions[33, 34]. Meanwhile, ECV can serve as a sensitive noninvasive imaging tool to observe changes in the extracellular space of the myocardium during diabetes progression and can be used to dynamically monitor the characteristic of the early stage of DCM. In our study, the ECV value gradually increased during diabetes progression. The ECV value at 12 weeks significantly differed between the T1DM and control groups; this finding is in line with that obtained for CVF. Our study showed that the ECV value was strongly correlated with CVF, and the postcontrast T1 value was moderately associated with the CVF value. The main reason is likely that the gadolinium agent (as an extracellular contrast agent) could not pass through the cell membrane and enter the cell; therefore, the postcontrast T1 value was mainly associated with the contrast agent concentration in the extracellular matrix, which is consistent with the findings of our previous studies[23, 29] and another study[28]. In addition, our study showed that the ECV value was higher than CVF, possibly because the CVF value reflects only the extracellular collagen fiber content, whereas the ECV value can also indicate mucus matrix, lipid, and necrosis components outside cells. In the early stage of DCM, pathophysiological changes can occur including oxidative stress, inflammatory reaction, edema, fatty degeneration of the heart, lipid deposition, and mild myocardial fibrosis[2]. Thus, the combination of these pathological processes leads to changes in cardiac morphology and function.

Several recent studies have shown that collagen fibers can prolong the native T1 value; thus, native T1 mapping without injecting contrast agents can be used to detect DMIF[35, 36]. This method does not need injecting a gadolinium contrast agent and is more convenient than the acquisition of the ECV value. Native T1 mapping can be used in patients with severe renal dysfunction and allergic constitution. In our study, a moderate correlation was observed between the CVF value and native T1 value in the T1DM group (T1DM r = 0.557 and T2DM r = 0.538). However, pathophysiological changes in DCM are complex including edema, fatty degeneration, hemorrhage, and collagen deposition, which can prolong or shorten the native T1 value in the myocardium. Therefore, the application of the native T1 value in the evaluation of DCM still needs to be studied in the future. Meanwhile, native T1ρ mapping, as an endogenous contrast technique, has been used for detecting myocardial fibrosis[37]. This technique does not require exogenous contrast agents, and in some studies, a positive correlation between T1ρ and ECV was observed[28, 38]. Thus, in our next study, native T1ρ mapping may be applied in DCM.

Limitations

The present study has some limitation. First, the number of experimental animals was low. However, the current case numbers are reasonable in our study and based on previous statistical calculations. To some extent, this may affect the calculation of some correlation coefficients. We found that the dispersion of data is relatively stable; thus, the exact r values were reliable in our study. Second, the thickness of MRI scanning was 1 mm. However, the thickness of the biopsy sectioning layer was only 5 μm. In terms of pathological detection corresponding to the acquisition of MR data, it was challenging to ensure that the layers were identical. However, in the early stage of DM, the main manifestation in each segment of the myocardium was diffuse fibrosis, with a relatively uniform distribution of interstitial fibers. Thus, the results are stable. The thickness of MRI scanning was hundred times higher than the thickness of the biopsy-sectioning layer. Therefore, although pathological detection was performed based on the acquisition of MR data, we could ensure that the positions used for two diagnostic methods were identical. In addition, different T1 values might be acquired using various MRI equipment and postprocessing station. However, we used the self-equipment software to calculate the ECV value with HCT correction and found stable results. Finally, this study was conducted only in mice models, whereas multiple complications are observed in patients with DCM including hypertension, valvular heart disease, and coronary heart disease. Future studies with large human samples are needed.

Conclusion

In our study, ECV was found to be a reliable and feasible imaging marker for quantitatively assessing dynamic DMIF changes in T1DM mice. In addition, ECV could accurately detect DMIF in the early stage and thus can be used as a potential imaging tool for early intervention in T1DM mice in the future.

Abbreviations

DMIF: Diffuse myocardial interstitial fibrosis, HF: heart failure, DM: diabetes mellitus, DCM: diabetic cardiomyopathy, CVD: cardiovascular diseases, CMRI: cardiac magnetic resonance imaging, ECV: extracellular volume fraction, CVF: collagen volume fraction, FS: fraction shortening, EF :ejection fraction, LV: Left ventricular, ANOVA: one-way analysis of variance, T1DM: type-1 diabetes mellitus, STZ: streptozotocin.

Declarations

Authors' contributions

Conception and design: HKZ,ZMF and LX. Analysis and interpretation: HKZ,CYS,LY,NZ,GQL,ZZ,YFG,DTL. Drafting of the manuscript: HKZ,CYS,ZMF and LX. Revising the manuscript for important intellectual content: HKZ, CYS,LY,NZ,GQL,ZZ,YFG,DTL, ZMF and LX. All authors read and approved the final manuscript.

Acknowledgements

Not applicable.

Competing interests

The authors declare that they have no competing interests.

Availability of data and materials

The datasets used and/or analyzed during the current study are available from

the corresponding author on reasonable request.

Consent for publication

Not applicable.

Ethics approval and consent to participate

The experimental procedures for mice were approved by the Ethics Committee of Laboratory Animals at the Capital Medical University of China (Permission Number:

AEEI-2018-020).

Funding

This study was supported by grants from National Natural Science Foundation of China (U1908211, 81771791)and a grant from the Capital's Funds for Health Improvement and Research Foundation of China (2020-1-1052). Beijing Hospitals Authority Youth Programme (QML20190607).

References

1. Murtaza G, Virk H U H, Khalid M, et al. Diabetic cardiomyopathy - A comprehensive updated review [J]. Prog Cardiovasc Dis, 2019,
2. Ritchie R H, Abel E D. Basic Mechanisms of Diabetic Heart Disease [J]. Circ Res, 2020, 126(11): 1501-25.
3. Gulsin G S, Athithan L, McCann G P. Diabetic cardiomyopathy: prevalence, determinants and potential treatments [J]. Ther Adv Endocrinol Metab, 2019, Mar 27,10:2042018819834869..
4. Chavali V, Tyagi S C, Mishra P K. Predictors and prevention of diabetic cardiomyopathy [J]. Diabetes Metab Syndr Obes, 2013 Apr 11,6:151-60.
5. Wong T C, Piehler K, Meier C G, et al. Association between extracellular matrix expansion quantified by cardiovascular magnetic resonance and short-term mortality [J]. Circulation, 2012, 126(10): 1206-16.
6. Ambale-Venkatesh B, Lima J A. Cardiac MRI: a central prognostic tool in myocardial fibrosis [J]. Nat Rev Cardiol, 2015, 12(1): 18-29.
7. Rijzewijk L J, van der Meer R W, Smit J W, et al. Myocardial steatosis is an independent predictor of diastolic dysfunction in type 2 diabetes mellitus [J]. J Am Coll Cardiol, 2008, 52(22): 1793-9.
8. Mewton N, Liu C Y, Croisille P, et al. Assessment of myocardial fibrosis with cardiovascular magnetic resonance [J]. J Am Coll Cardiol, 2011, 57(8): 891-903.
9. Roy C, Slimani A, de Meester C, et al. Associations and prognostic significance of diffuse myocardial fibrosis by cardiovascular magnetic resonance in heart failure with preserved ejection fraction [J]. J Cardiovasc Magn Reson, 2018, 20(1): 55.
10. Xu Z, Wang S, Ji H, et al. Broccoli sprout extract prevents diabetic cardiomyopathy via Nrf2 activation in db/db T2DM mice [J]. Sci Rep, 2016 Jul 26,6:30252.
11. Gu J, Cheng Y, Wu H, et al. Metallothionein Is Downstream of Nrf2 and Partially Mediates Sulforaphane Prevention of Diabetic Cardiomyopathy [J]. Diabetes, 2017, 66(2): 529-42.
12. Bai Y, Cui W, Xin Y, et al. Prevention by sulforaphane of diabetic cardiomyopathy is associated with up-regulation of Nrf2 expression and transcription activation [J]. J Mol Cell Cardiol, 2013 Apr,57:82-95.
13. Cai L, Wang J, Li Y, et al. Inhibition of superoxide generation and associated nitrosative damage is involved in metallothionein prevention of diabetic cardiomyopathy [J]. Diabetes, 2005, 54(6): 1829-37.
14. Matyas C, Kovacs A, Nemeth B T, et al. Comparison of speckle-tracking echocardiography with invasive hemodynamics for the detection of characteristic cardiac dysfunction in type-1 and type-2 diabetic rat models [J]. Cardiovasc Diabetol, 2018, 17(1): 13.
15. Price A N, Cheung K K, Lim S Y, et al. Rapid assessment of myocardial infarct size in rodents using multi-slice inversion recovery late gadolinium enhancement CMR at 9.4T [J]. J Cardiovasc Magn Reson, 2011, 13(1): 44.
16. Stuckey D J, McSweeney S J, Thin M Z, et al. T mapping detects pharmacological retardation of diffuse cardiac fibrosis in mouse pressure-overload hypertrophy [J]. Circ Cardiovasc Imaging, 2014, 7(2): 240-9.
17. Taylor A J, Gutman S J. Myocardial T1 Mapping in Heart Disease: Research Tool or New Cardiac Biomarker? [J]. JACC Cardiovasc Imaging, 2020, 13(1 Pt 1): 55-7.
18. Boudina S, Abel E D. Diabetic cardiomyopathy revisited [J]. Circulation, 2007, 115(25): 3213-23.
19. Doltra A, Stawowy P, Dietrich T, et al. Magnetic resonance imaging of cardiovascular fibrosis and inflammation: from clinical practice to animal studies and back [J]. Biomed Res Int, 2013,2013:676489.
20. Santos A, Fernández-Friera L, Villalba M, et al. Cardiovascular imaging: what have we learned from animal models? [J]. Front Pharmacol, 2015 Oct 21,6:227.
21. Verkaik M, van Poelgeest E M, Kwekkeboom R F J, et al. Myocardial contrast echocardiography in mice: technical and physiological aspects [J]. Am J Physiol Heart Circ Physiol, 2018, 314(3): H381-h91.
22. Blomstrand P, Engvall M, Festin K, et al. Left ventricular diastolic function, assessed by echocardiography and tissue Doppler imaging, is a strong predictor of cardiovascular events, superior to global left ventricular longitudinal strain, in patients with type 2 diabetes [J]. Eur Heart J Cardiovasc Imaging, 2015, 16(9): 1000-7.
23. Zeng M, Qiao Y, Wen Z, et al. The Association between Diffuse Myocardial Fibrosis on Cardiac Magnetic Resonance T1 Mapping and Myocardial Dysfunction in Diabetic Rabbits [J]. Sci Rep, 2017 Mar 24,7:44937.
24. Markman T M, Habibi M, Venkatesh B A, et al. Association of left atrial structure and function and incident cardiovascular disease in patients with diabetes mellitus: results from multi-ethnic study of atherosclerosis (MESA) [J]. Eur Heart J Cardiovasc Imaging, 2017, 18(10): 1138-44.
25. Jensen M T, Fung K, Aung N, et al. Changes in Cardiac Morphology and Function in Individuals With Diabetes Mellitus: The UK Biobank Cardiovascular Magnetic Resonance Substudy [J]. Circ Cardiovasc Imaging, 2019, 12(9): e009476.
26. Espe E K, Aronsen J M, Eriksen G S, et al. Assessment of regional myocardial work in rats [J]. Circ Cardiovasc Imaging, 2015, 8(2): e002695.
27. Hu X, Bai T, Xu Z, et al. Pathophysiological Fundamentals of Diabetic Cardiomyopathy [J]. Compr Physiol, 2017, 7(2): 693-711.

28. Zhang Y, Zeng W, Chen W, et al. MR extracellular volume mapping and non-contrast T1rho mapping allow early detection of myocardial fibrosis in diabetic monkeys [J]. Eur Radiol, 2019, 29(6): 3006-16.
29. Zeng M, Zhang N, He Y, et al. Histological validation of cardiac magnetic resonance T1 mapping for detecting diffuse myocardial fibrosis in diabetic rabbits [J]. J Magn Reson Imaging, 2016, 44(5): 1179-85.
30. Bergerot C, Davidsen E S, Amaz C, et al. Diastolic function deterioration in type 2 diabetes mellitus: predictive factors over a 3-year follow-up [J]. Eur Heart J Cardiovasc Imaging, 2018, 19(1): 67-73.
31. Stuckey D J, McSweeney S J, Thin M Z, et al. T(1) mapping detects pharmacological retardation of diffuse cardiac fibrosis in mouse pressure-overload hypertrophy [J]. Circ Cardiovasc Imaging, 2014, 7(2): 240-9.
32. Gao Y, Yang Z G, Ren Y, et al. Evaluation myocardial fibrosis in diabetes with cardiac magnetic resonance T1-mapping: Correlation with the high-level hemoglobin A1c [J]. Diabetes Res Clin Pract, 2019 Apr,150:72-80.
33. Cao Y, Zeng W, Cui Y, et al. Increased myocardial extracellular volume assessed by cardiovascular magnetic resonance T1 mapping and its determinants in type 2 diabetes mellitus patients with normal myocardial systolic strain [J]. Cardiovasc Diabetol, 2018, 17(1): 7.
34. Robinson A A, Chow K, Salerno M. Myocardial T1 and ECV Measurement: Underlying Concepts and Technical Considerations [J]. JACC Cardiovasc Imaging, 2019, 12(11 Pt 2): 2332-44.
35. Sado D M, Maestrini V, Piechnik S K, et al. Noncontrast myocardial T1 mapping using cardiovascular magnetic resonance for iron overload [J]. J Magn Reson Imaging, 2015, 41(6): 1505-11.
36. Nakamori S, Fahmy A, Jang J, et al. Changes in Myocardial Native T(1) and T(2) After Exercise Stress: A Noncontrast CMR Pilot Study [J]. JACC Cardiovasc Imaging, 2020, 13(3): 667-80.
37. Wang C, Zheng J, Sun J, et al. Endogenous contrast T1rho cardiac magnetic resonance for myocardial fibrosis in hypertrophic cardiomyopathy patients [J]. J Cardiol, 2015, 66(6): 520-6.
38. Yin Q, Abendschein D, Muccigrosso D, et al. A non-contrast CMR index for assessing myocardial fibrosis [J]. Magn Reson Imaging, 2017 Oct,42:69-73.

Tables

Table 1. Basic characteristic and echocardiographic parameters of the control and T1DM groups

Time（Weeks）	Baseline		4		8		12	
Groups	control	T1DM	control	T1DM	control	T1DM	control	T1DM
HR(bpm)	392±32	389±36	394±36	382±37	390±33	383±26	396±29	404±30
Resp(Breath/min)	35±3	33±4	37±4	33±2	38±4	36±4	38±3	37±3
A wave(mm/s)	339.17±28.2	314.67±12.15	342.75±19.78	357.15±26.06	365.59±23.64	369.02±19.19	353.38±27.41	429.16±26.71
E wave(mm/s）	709.97±26.25	696.4±17.04	710.64±14.63	699.08±18.83	713.24±11.84	697.56±19.43	709.95±16.55	659.14±11.65
E/A(radio)	2.1±0.15	2.22±0.13	2.08±0.11	1.97±0.15	1.96±0.14	1.87±0.1	2.02±0.16	1.54±0.07*
LVEF(%)	69.39±1.56	68.38±2.94	68.67±2.72	67.14±3.58	67.29±2.96	64.41±4.56	66.92±3.5	62.91±2.76
FS(%)	42.38±1.79	45.07±2.45	42.94±1.72	43.7±3.14	41.51±2.36	44.33±3.68	41.93±1.69	40.25±2.8
LV mass(mg)	97.9±3.09	94.28±6.42	99.07±4.54	100.09±8.84	101.71±6.16	112.82±12.56	106.35±8.65	120.09±10.42
LV mass (Corrected, mg)	77.39±2.19	76.19±3.42	78.02±3.92	80.08±7.07	80.03±4.8	86.96±7.84	85.82±7.51	96.74±7.82*

The table shows the parameters of the control and T1DM groups from baseline to 24 weeks. Values are presented as mean ± SD. Heart rate(HR),respiration(Resp),left ventricle (LV),ejection fraction (EF), fractional shortening (FS).

*P < 0.05 vs control mice at the same time point. #P< 0.05 vs T1DM 12weeks mice (A wave, E wave, E/A radio, LV mass and LV mass (Corrected)).

&P< 0.05 vs T1DM 16weeks mice (LVEF and FS).

Figures

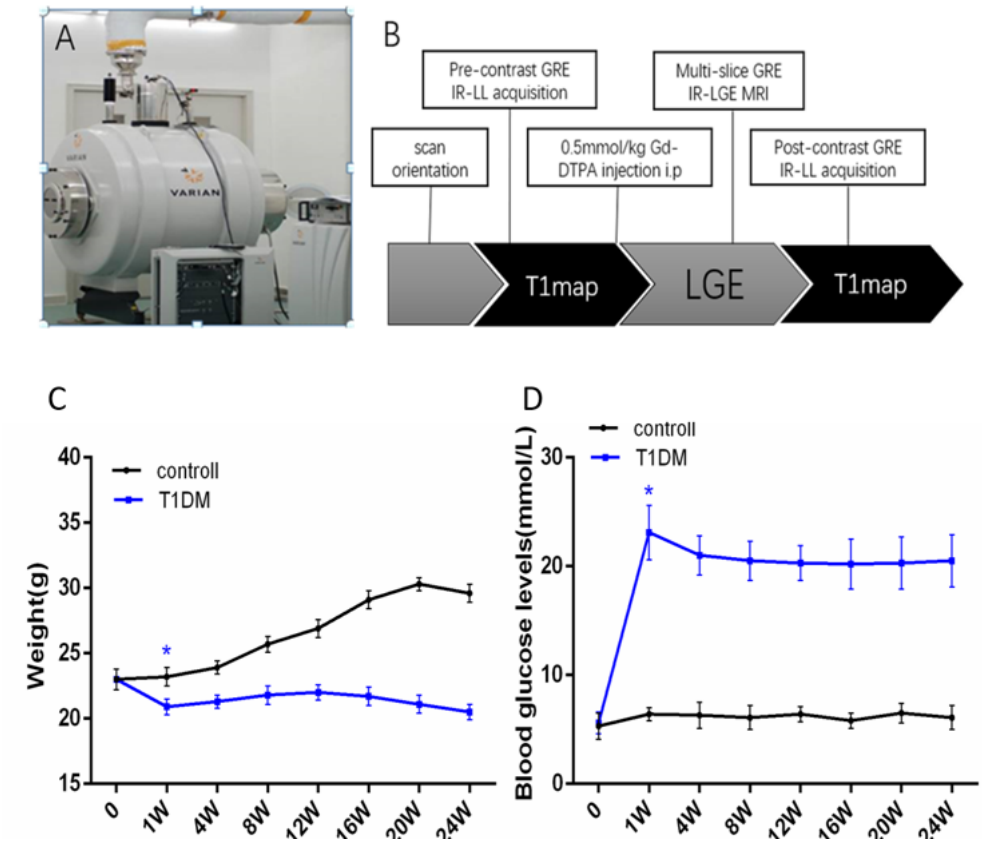

Figure 1

7.0 T MRI system (A) from Varian. B, MRI acquisition protocol (B) for control and T1DM groups. Comparison of average weight (C) and blood glucose levels (D) between control and T1DM groups from 0 to 24 weeks. At each time, six mice were randomly chosen from each group, and the mean ± standard deviation are plotted as dots and bars, respectively. *p < 0.001 versus control 1W mice (T test). IR-LL = inversion recovery look–locker, LGE-MRI = late-gadolinium enhancement magnetic resonance imaging

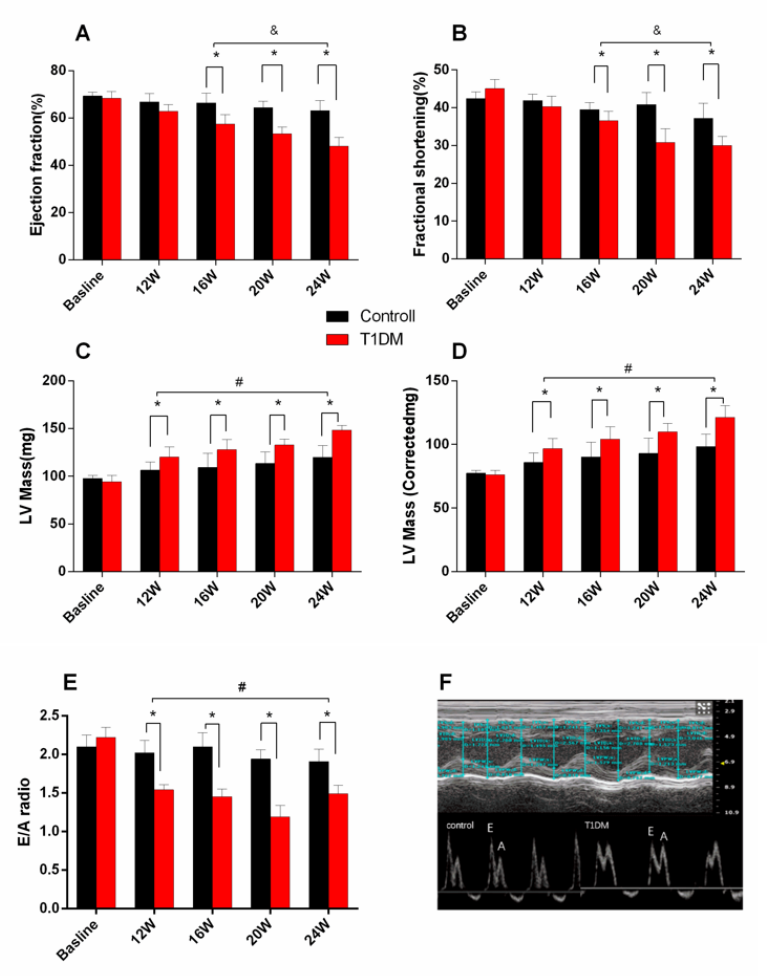

Figure 2

Cardiac structure and function in control and T1DM groups from baseline to 24 weeks. (A) Ejection fraction (EF). (B) Fractional shortening (FS). (C) LV mass. (D) LV mass (corrected). (E) E/A ratio and (F) acquired by M-mode echocardiography. Data are presented as the mean ± standard deviation at the same time point (t test), and differences between two groups were examined using ANOVA. (n = 5 or 6). *P < 0.05 vs control mice at the same time point. #P< 0.05 vs T1DM mice at 12 weeks (E/A ratio, LV mass, and LV mass [corrected]). &P< 0.05 vs T1DM mice at 16 weeks (LVEF and FS).

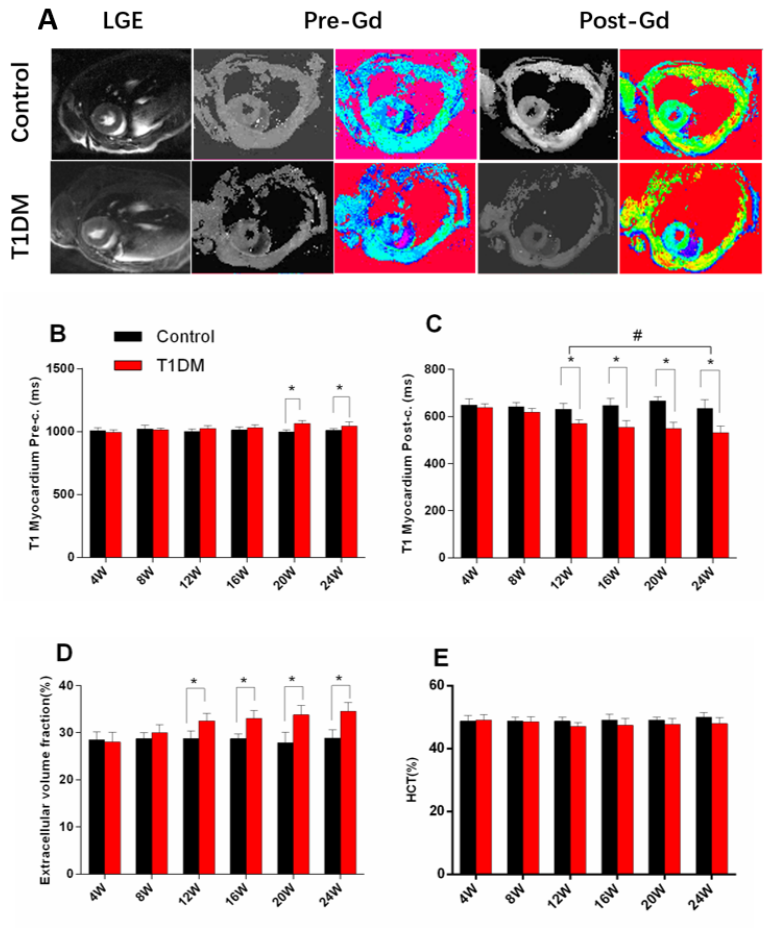

Figure 3

A bar plot for myocardial T1, blood values, and ECV in control and T1DM groups from 4 to 24 weeks. (A) LGE, pre- and post-contrast T1 maps from control and T1DM groups at 12 weeks. Color scale bar shows a T1 value from 0 to 2000 ms. (B) Precontrast myocardial T1 times. (C) Postcontrast myocardial T1 times. (D) Extracellular volume fraction (ECV). (E) Hematocrit (HCT). Data are presented as the mean ± standard deviation (n = 6). (t test), Differences between two groups were examined using ANOVA. *P < 0.05 vs control mice at the same time point., #P< 0.05 vs T1DM mice at 12 weeks (T1 myocardium post-c.).

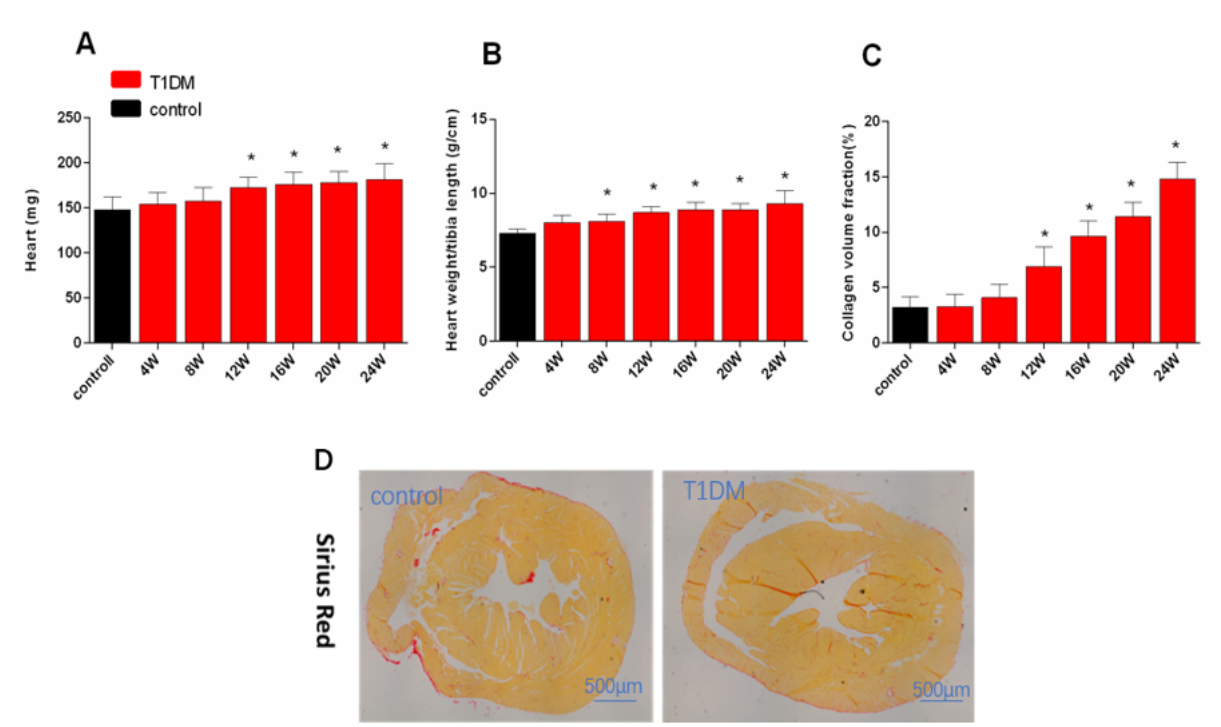

Figure 4

A bar plot for the heart weight (A) and the ratio of heart weight/tibia length (B) and collagen volume fraction (C) in control and T1DM groups. Sirius Red staining (D) (red = fibrosis and orange = myocardial fibers): Comparison with the control group, diffuse interstitial fibrosis became increasingly severe in the T1DM group at 12 weeks. Data are presented as the mean ± standard deviation (n = 3) and *P < 0.05 vs control mice at the same time point (t test). ANOVA was used to examine differences between the two groups.

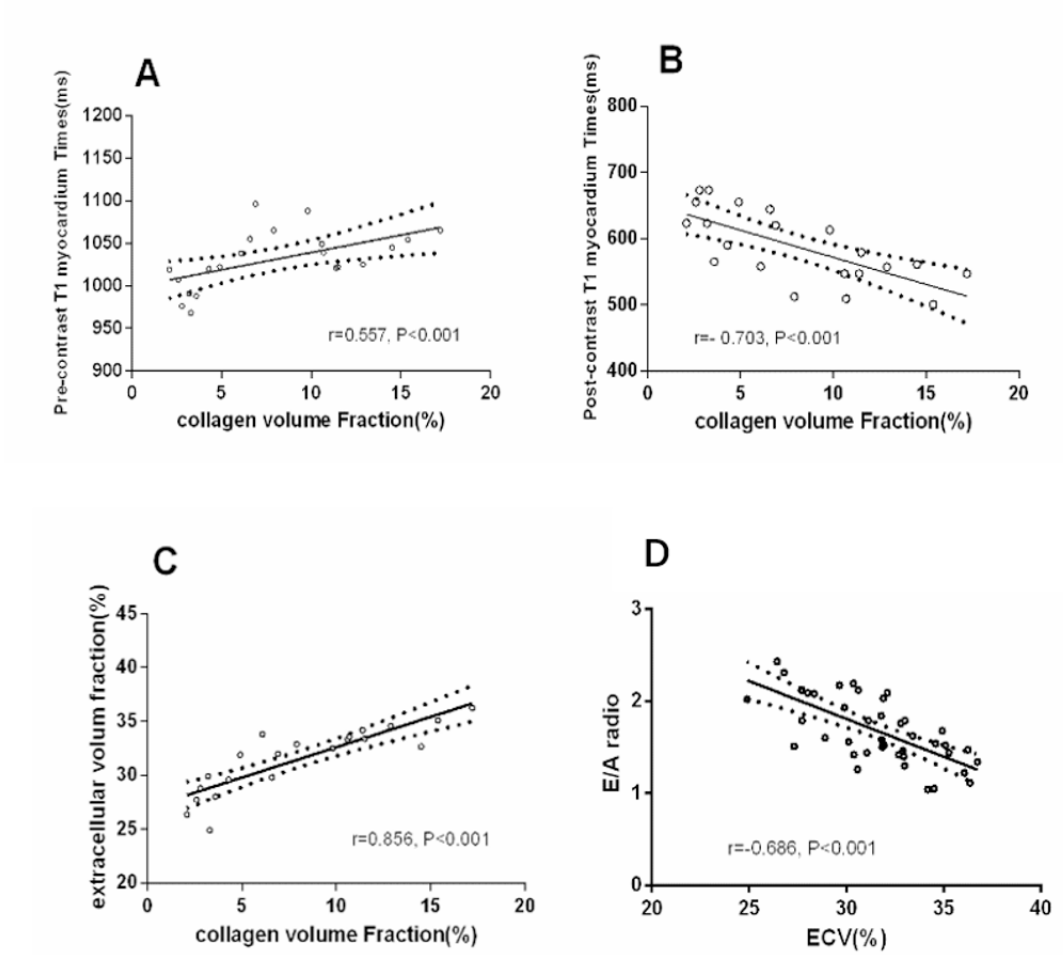

Figure 5

Correlations between histological myocardial fibrosis and cardiac MR quantification of T1 mapping in control and T1DM groups from each timepoint. Correlation between precontrast and postcontrast myocardial T1 times, ECV, and collagen volume fraction (CVF) in T1DM (A,B,C). Correlation between the E/A ratio and ECV in T1DM (D).